BJR

https://doi.org/10.1259/bjr.20170805

Received: 18 October 2017 | Revised: 09 March 2018 | Accepted: 23 March 2018

Cite this article as:
Hwang EJ, Kim H, Park CM, Yoon SH, Lim H, Goo JM. Cone beam computed tomography virtual navigation-guided transthoracic biopsy of small (≤ 1 cm) pulmonary nodules: impact of nodule visibility during real-time fluoroscopy. *Br J Radiol* 2018; **91**: 20170805.

FULL PAPER

Cone beam computed tomography virtual navigation-guided transthoracic biopsy of small (≤ 1 cm) pulmonary nodules: impact of nodule visibility during real-time fluoroscopy

[1]EUI JIN HWANG, MD, [1]HYUNGJIN KIM, MD, [1,2]CHANG MIN PARK, MD, PhD, [1,2]SOON HO YOON, MD, [3]HYUN-JU LIM, MD, PhD and [1,2]JIN MO GOO, MD, PhD

[1]Department of Radiology, Seoul National University College of Medicine, Seoul, Korea
[2]Institute of Radiation Medicine, Seoul National University Medical Research Center, Seoul, Korea
[3]Department of Radiology, National Cancer Center, Goyang-si, Gyeonggi-do, Korea

Address correspondence to: Dr Chang Min Park
E-mail: *cmpark.morphius@gmail.com*

The authors Eui Jin Hwang and Hyungjin Kim contributed equally to the work.

Objective: To evaluate the impact of nodule visibility during real-time fluoroscopy and other biopsy-related variables on the diagnostic accuracy and complication rates of cone beam CT (CBCT) virtual navigation (VN)-guided percutaneous transthoracic needle biopsies (PTNBs) of small (≤1 cm) pulmonary nodules.

Methods: Patients (99 males and 114 females; age, 62.1 ± 11.1 years) who underwent CBCT VN-guided biopsies for lung nodules ≤ 1 cm were retrospectively reviewed. The visibility of target nodules was assessed on the captured fluoroscopy images. Diagnostic accuracies were calculated and logistic regression analyses were performed to determine independent influencing factors for the correct diagnosis and complications (pneumothoraxes and hemoptysis) in CBCT VN-guided PTNBs, respectively.

Results: Among 213 nodules, 63 (29.6%) were invisible on real-time fluoroscopy during VN. The diagnostic accuracy of CBCT VN-guided PTNBs for the invisible nodules was 76.7%, while for the visible nodules was 89.1% (p = 0.042). In the logistic regression analysis, the visibility of a target nodule (odds ratio = 2.49, p = 0.047) was the only independent influencing factor for a correct diagnosis. As regards complication rates, nodule visibility was not a significant factor for the occurrence of a pneumothorax or hemoptysis.

Conclusion: Although nodule visibility on real-time fluoroscopy was an affecting factor for the correct diagnosis, CBCT VN-guided PTNB was feasible for the invisible nodules with diagnostic accuracy of 76.7%.

Advance in knowledge: CBCT VN-guided PTNB can be tried safely for the subcentimeter-sized pulmonary nodules regardless of their fluoroscopic visibility.

INTRODUCTION

Increased utilization of low-dose CT in lung cancer screening resulted in a sharp rise in the number of small nodules detected.[1,2] In the National Lung Screening Trial, 22.0% of participants at baseline had nodules ≤ 1 cm. In addition, 19.6 and 34.5% of lung cancers detected on low-dose CT were 1 cm or smaller in diameter at baseline and at first annual repeat screening, respectively.[3,4] Recent guidelines recommend that a biopsy should be considered in cases of indeterminate lung nodules ≥ 8 mm.[5–7] In this context, the demand for the biopsy of small nodules will gradually increase.

State-of-the-art cone beam CT (CBCT) system offers virtual navigation (VN) guidance for a percutaneous transthoracic needle biopsy (PTNB). CBCT-guided PTNB has shown excellent diagnostic performance for the small lung nodules.[8–11] CBCT VN enables automatic angulation of the X-ray tube and vertical alignment between the tube and a target. Thus, an operator can easily insert a needle through a pre-planned path targeting a virtual color marking on real-time fluoroscopy. Theoretically, a tangentially inserted needle through the pre-determined path should reach the target nodule. However, the virtual needle pathway is reconstructed based on the pre-procedural CBCT scan, which are

static CT images. Respiratory motion may hamper the registration between the virtual color marking and the real target. Therefore, in such case, the target nodule should be tracked visually by the operator on real-time fluoroscopy during needle insertion through the respiratory cycles. The predetermined needle pathway has to be adjusted to take account of the movement of the target lesion caused by respiration.

For the subcentimeter-sized nodules, visual tracking of nodules on real-time fluoroscopy may not be feasible as they are often invisible due to the surrounding structures (diaphragm or heart), obscuring lung parenchymal abnormality, low nodule density (subsolid nodules) or very small nodule size. Diagnostic accuracy of CBCT VN-guided biopsy can be unexpectedly low in these nodules and PTNB may not be a useful modality in this setting. However, to our knowledge, there has been no investigation with respect to the effect of the fluoroscopic nodule visibility on the diagnostic accuracy and safety of CBCT VN-guided biopsies for the small nodules.

Thus, in this study, we aimed to evaluate the impact of the nodule visibility during real-time fluoroscopy for needle insertion and other biopsy-related variables on the diagnostic accuracy and complication rates of CBCT VN-guided PTNBs of small (≤1 cm) pulmonary nodules.

METHODS AND MATERIALS

The present study was approved by the Institutional Review Board of Seoul National University Hospital, and written informed consent was waived.

Patient selection

Based on electronic medical records (EMRs), a total of 242 consecutive patients (118 males and 124 females) aged (mean ± standard deviation) 61.5 ± 11.6 years (range, 27–84 years) were initially included according to the following inclusion criteria: (a) patients who underwent CBCT VN-guided PTNBs for lung nodules between January 2012 and December 2016; (b) patients with complete procedural reports written by the operators; and (c) patients who had lung nodules with a unidimensional diameter ≤1 cm on preprocedural CBCT images. Among the patients initially selected, 29 were excluded from the study according to the following exclusion criteria: (a) repeat PTNBs (n = 6) and (b) patients without appropriately captured intraprocedural fluoroscopic images (n = 23). Finally, 213 patients (males, n = 99; females, n = 114) aged 62.1 ± 11.1 years (range, 27–84 years) were included in this study. Figure 1 presents a flow diagram of patient inclusion and exclusion. The median size of the target nodules was 1.0 cm (size range, 0.5–1.0 cm). Among the study population, 51 patients (23.9%) were included in our past publication.[12]

CBCT VN-guided PTNB

All biopsies were performed using one of the three CBCT systems (Artis Zee and Axiom Artis, Siemens Healthcare, Erlangen, Germany; Allura Xper FD20, Philips Healthcare, Best, Netherlands), with the aid of dedicated virtual guidance software programs [Syngo i-Guide, Siemens Healthcare (Best, Netherlands); XperGuide, Philips Healthcare (Best, Netherlands)]. Prior to PTNBs, all patients underwent pre-procedural planning CBCTs at full expiration. After review of the

Figure 1. Patient inclusion and exclusion flow diagram. Initially, 242 patients who underwent CBCT virtual navigation-guided PTNB for lung nodules ≤ 1 cm between January 2012 and December 2016 were retrospectively included. After exclusion of six patients who underwent repeat biopsies and 23 patients without appropriately captured fluoroscopic images, 213 patients were finally included. In the diagnostic accuracy assessment, 41 patients with biopsy results of atypical cells and indeterminate results according to gold standards were further excluded. CBCT, cone beam CT; PTNB, percutaneous transthoracic needle biopsy.

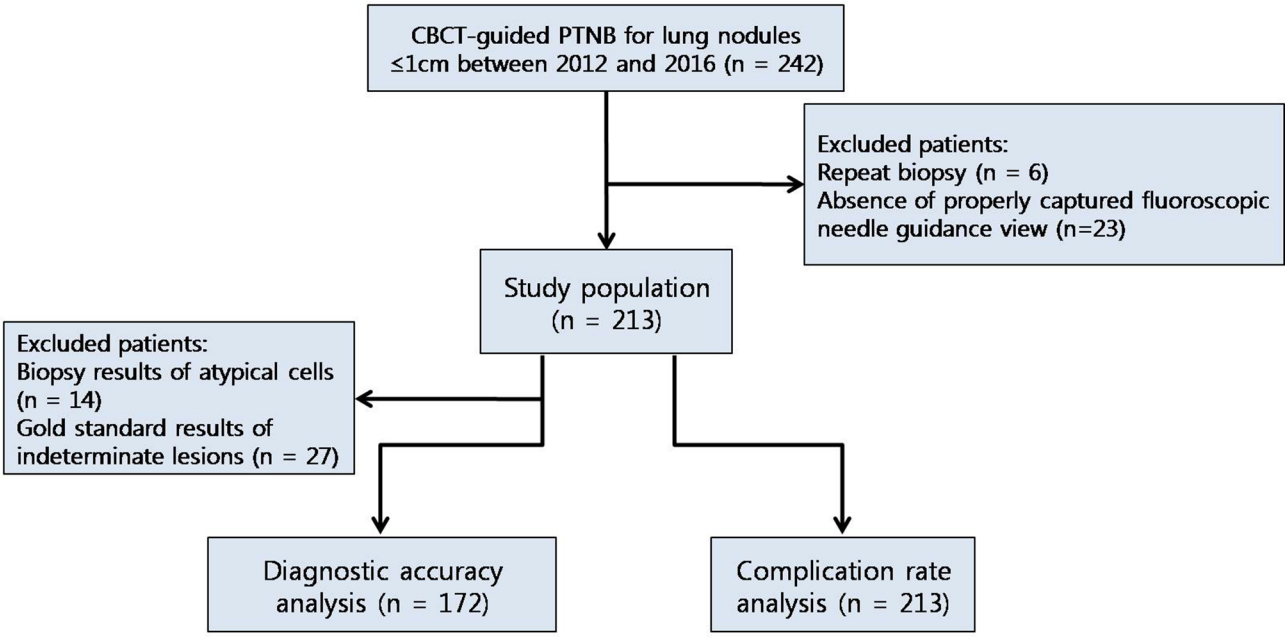

Figure 2. An example of CBCT virtual navigation-guided PTNB using virtual guidance software. Based on the preprocedural CBCT images, the operator determined the safest virtual needle pathway, specifying the skin entry site and virtual location of the needle tip (a). The C-arm automatically rotated in the direction of the virtual needle pathway and that of the X-ray, providing a fluoroscopic needle guidance view (bull's eye view, b). The actual location of the needle tip was confirmed by intraprocedural CBCT (c). After tissue acquisition and removal of the needle, a postprocedural CBCT scan was obtained to check for the occurrence of complications (d).

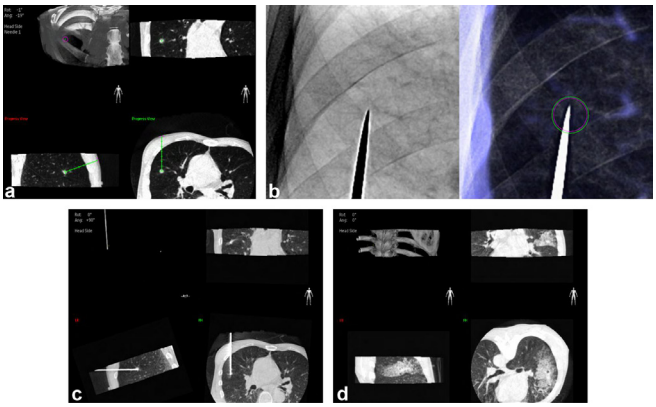

pre-procedural CBCTs and conventional diagnostic CT scans taken before the procedure, operators determined the optimal pathway on pre-procedural CBCT scans to maximize the diagnostic yield of PTNB and minimize the risk of complications. Virtual needle pathway to the target on the pre-procedural CBCT images was determined and vertical alignment from the skin entry site to the target lesion was set automatically, with color spot marking on the fluoroscopic image (bull's eye view). The needle was then inserted under fluoroscopy guidance. Needle insertion was routinely done under breath-hold after full expiration to optimize the registration between pre-procedural CBCT and fluoroscopy. If an appropriate needle pathway could not be secured in the expiration status, planning was conducted again at full inspiration state with repeat CBCT scanning. All biopsy procedures were performed by or under the supervision of one of the two thoracic radiologists (CMP and SHY, with 11 and 4 years of experience in thoracic interventions, respectively). Coaxial core biopsies were performed with 17-gauge introducers and 18-gauge cutting biopsy needles or with 18-gauge introducers and 20-gauge needles (Stericut, TSK Laboratory, Japan). Aspiration biopsies were performed with 22-gauge needles (Westcott, Argon Medical Devices, TX). A core biopsy was initially considered in all cases in accordance with our institutional protocol. Aspiration was an option in cases of necrotic nodules or lesions deemed to be of too high risk for a core biopsy. Figure 2 shows an example of a biopsy procedure.

Data collection

Patient-related data (gender and age) were obtained from the EMRs. Biopsy-related data [size, characteristics and location of the target nodule, pleura-to-target distance (PTTD), core biopsy *vs* aspiration biopsy, needle indwelling time, and total procedure time] and data on complications (pneumothorax and hemoptysis) were acquired from the operators' structured reports for the PTNB procedures.

The visibility of nodules on the fluoroscopy was retrospectively evaluated using the bull's eye view images, which were routinely saved during the procedure. Two radiologists (HK and EJH, with 8 and 7 years of experience in chest radiology, respectively) who were blinded to the biopsy results and final diagnoses independently assessed the visibility of the nodules.

Measurements and definitions

Age: the patients were categorized into two age groups: (a) 60 years old or younger and (b) older than 60 years.

Patient's position: patient's position during the PTNB procedures (*i.e.* supine or prone position) was recorded.

Target size: the largest diameter of the target nodule was measured on axial preprocedural CBCT images.

Target characteristics: the target nodules were classified into two groups based on a review of the preprocedural CT: (a) solid and (b) subsolid.

Target location: the location of the nodule was classified as (a) upper or middle lobe and (b) lower lobe.

PTTD: the distance between the pleural puncture site and target nodule along the needle track on reformatted CBCT images was defined as the PTTD. PTTD was dichotomized as follows: (a) shallow location (*i.e.* PTTD ≤2 cm) and (b) deep location (*i.e.* PTTD >2 cm).

Presence of emphysema: any presence of emphysema in the background lung parenchyma was recorded based on a review of the preprocedural CT.

Biopsy method: the biopsy method (*i.e.* a core needle biopsy or fine needle aspiration) was recorded.

Needle indwelling time and total procedure time: the needle indwelling time was defined as the time interval between the needle introduction through the skin and removal of the needle from the patient. The total procedure time was defined as the time interval between local anesthesia injection and end of the acquisition of postprocedural CBCT.

Occurrence of a pneumothorax: a pneumothorax was defined as the presence of any air in the pleural space on postprocedural CBCT or subsequent chest radiographs.

Occurrence of hemoptysis: any expectoration of blood-tinged sputum or fresh blood after the procedure was considered as hemoptysis.

Assessment of diagnostic accuracy

For the evaluation of diagnostic accuracy, pathological reports of PTNB specimens and EMRs were reviewed. Pathological reports

Figure 3. Examples of invisible nodules on real-time fluoroscopy. Nodule invisibility was caused by obscuring structures, such as the clavicle (a) or heart (b), and underlying parenchymal lung disease (usual interstitial pneumonia; c).

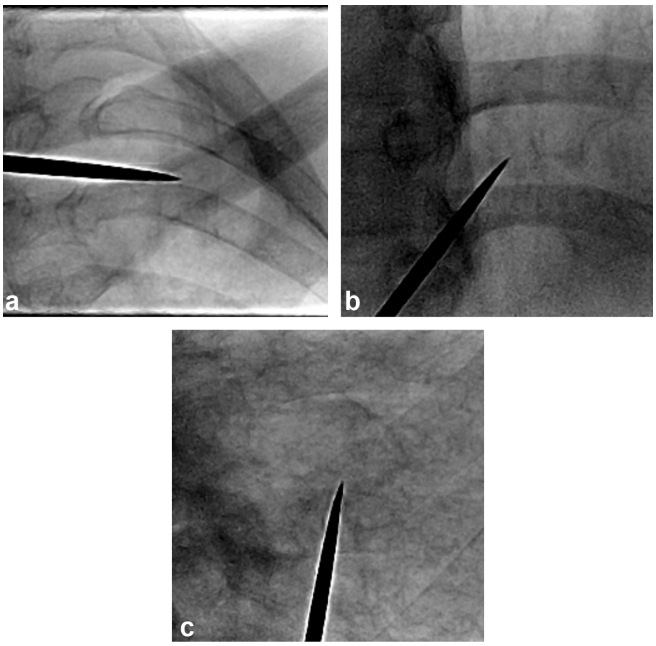

(biopsy results) were classified into five categories: (a) malignancy (primary lung cancer or metastasis); (b) atypical cells (presence of atypical cells without a definitive diagnosis of malignancy); (c) specific benign pathology (*e.g.* hamartoma, tuberculosis, or cryptococcosis); (d) non-specific benign pathology (*e.g.* chronic inflammation with fibrosis or chronic granulomatous inflammation); and (e) non-diagnostic specimen (*e.g.* tissue insufficient for diagnosis or necrotic tissue only). In the final diagnoses (gold-standards), the lesions were classified into three categories: (a) malignant, (b) benign, or (c) indeterminate. Malignant and specific benign pathology either on the PTNB or surgical resection were considered as the final diagnoses. Lesions with non-specific benign pathology were considered benign if they decreased on follow-up studies or remained stable for more than 2 years. Lesions not classified as either malignant or benign were regarded as indeterminate. Patients with malignant biopsy results followed by a diagnosis of malignancy (true-positive) according to gold-standards and those with benign biopsy results followed by a diagnosis of benign (true-negative) according to gold-standards were classified as having a correct diagnosis. On the other hand, patients with benign biopsy results followed by a diagnosis of malignancy (false-negative) according to gold-standards were classified as having an incorrect diagnosis. Patients with non-diagnostic specimens were also classified as having an incorrect diagnosis, regardless of gold-standards. Cases with biopsy results of atypical cells (n = 14) and indeterminate final diagnoses (n = 27) were excluded from the diagnostic accuracy analysis.

Statistical analysis

To assess the inter-reader agreement of fluoroscopic nodule visibility, Cohen's κ statistic was calculated,[13] and the McNemar test was performed subsequently to check for differences in the visibility assessments of the two readers.

Diagnostic accuracy of PTNB was calculated for the overall population as well as for the fluoroscopically visible and invisible nodules, respectively. Then, X^2 tests were performed for the cross-table analyses. The Kolmogorov–Smirnov test was performed to assess the normality of continuous variables. The Student's t-test or Mann–Whitney U test was conducted to compare continuous variables. Binary logistic regression analyses were performed to identify factors associated with correct biopsy results and the occurrence of pneumothoraxes and hemoptysis. Following a univariable logistic regression analysis of each candidate factor, forward stepwise multivariable logistic regression analyses were performed using candidate factors that showed a p-value < 0.1 in the univariable analyses. Results with p-values < 0.05 were considered statistically significant. All statistical analyses were performed using IBM SPSS statistics (v. 23.0, IBM, Armonk, NY).

RESULTS

The percentage of fluoroscopically invisible nodules was 29.6% (63/213) for Reader 1 and 31.0% (66/213) for Reader 2. The percentage of inter-reader agreement on the fluoroscopic nodule visibility was 93.4% (199/213). Cohen's κ was 0.83 [excellent agreement; 95% confidence interval (CI), (0.75–0.91)].[13] There was no significant difference in the nodule visibility assessment between the two readers (p = 0.238). Therefore, the following statistical outcomes were based on the visibility assessment results of the Reader 1.[14]

Several factors resulted in the invisibility of small nodules on real-time fluoroscopy. These included obscuring structures, parenchymal lung opacity (interstitial lung disease), and the patient's body habitus (Figure 3). Table 1 shows the demographics and procedure-related variables of the patients with visible and invisible target nodules on fluoroscopy, respectively.

Based on the gold-standards, there were 118 (55.4%) malignant nodules (56 primary lung cancers and 62 metastases), 63 (29.6%) benign nodules, and 32 (15.0%) indeterminate nodules. Among 63 benign nodules, 23 were pathologically confirmed as specific benign pathology, 28 decreased in size or disappeared on follow-up CT, and the other 12 remained stable for more than 2 years.

Diagnostic accuracy

Among 172 PTNB cases included in the diagnostic accuracy analysis (83 males and 89 females aged 61.4 ± 11.07 years; age range, 27–83 years), true positive, true negative, and false negative results were found in 89, 59, and 24 cases, respectively. In the false negatives, there were four cases of nondiagnostic specimens.

The diagnostic accuracy for overall population was 86.0% [95% CI (80.1–90.4%)]. For the invisible nodules on fluoroscopy, the diagnostic accuracy was 76.7% and this was significantly lower than that for the visible nodules (89.1%; p = 0.042). Table 2 shows the results of the univariable analyses of the diagnostic accuracy. The nodule visibility was the only significant influencing

Table 1. Comparisons between the patients with visible and invisible target nodules on fluoroscopy

Variable	Visible nodules (n = 150)	Invisible nodules (n = 63)	p-value
Gender			0.605[c]
Male	68 (45.3%)	31 (49.2%)	
Female	82 (54.7%)	32 (50.8%)	
Age[a]	61.8 ± 11.3	62.9 ± 10.9	0.500[d]
Age ≤ 60 years	72 (48.0%)	24 (38.1%)	0.185[c]
Age > 60 years	78 (52.0%)	39 (61.9%)	
Patient's position			0.339[c]
Prone	97 (64.7%)	45 (71.4%)	
Supine	53 (35.3%)	18 (28.6%)	
Target size (cm)[b]	0.9 (0.5–1.0)	1.0 (0.5–1.0)	0.146[e]
Target location			0.086[c]
Upper or middle lobe	91 (60.7%)	46 (73.0%)	
Lower lobe	59 (39.3%)	17 (27.0%)	
Target characteristics			0.124[c]
Solid	146 (97.3%)	59 (93.7%)	
Subsolid	4 (2.7%)	4 (6.3%)	
PTTD (cm)[b]	1.6 (0–7.3)	2.0 (0–7.2)	0.069[e]
PTTD ≤ 2 cm	90 (60.0%)	32 (50.8%)	0.215[c]
PTTD > 2 cm	60 (40.0%)	31 (49.2%)	
Biopsy method			0.840[c]
Core needle biopsy	147 (98.0%)	62 (98.4%)	
Fine needle aspiration	3 (2.0%)	1 (1.6%)	
Presence of emphysema	16 (10.7%)	9 (14.3%)	0.454[c]
Needle indwelling time (minute)[b]	8 (3–39)	9 (4–36)	0.519[e]
Total procedure time (minute)[b]	11 (6–42)	11 (6–39)	0.487[e]
Diagnostic accuracy			0.042[c]
Accurate diagnosis	115 (89.1%)	33 (76.7%)	
Inaccurate diagnosis	14 (10.9%)	10 (23.3%)	

PTTD, pleura-to-target distance.
[a]Data are mean ± standard deviation.
[b]Data are median (range)
[c]X^2 test.
[d]Student's t-test.
[e]Mann–-Whitney U test.

factor for a correct diagnosis [odds ratio (OR) = 2.49; 95% CI (1.01–6.12); p = 0.047]. Among four nodules with nondiagnostic specimens, one was invisible on fluoroscopy and biopsied by fine needle aspiration, while the other three visible nodules were sampled by core biopsy.

Figures 4 and 5 show representative cases of CBCT VN-guided PTNBs for visible and invisible targets, respectively.

Occurrence of a pneumothorax

A pneumothorax occurred in 62 of 213 (29.1%) cases. Percutaneous drainage catheters or chest tubes were inserted in 4 (1.9%) cases. In the χ^2 analysis, nodule visibility showed no significant association with the occurrence of a pneumothorax (p = 0.226). Table 3 shows the results of the univariable analyses of pneumothorax occurrence. Patient age, PTTD, and presence of emphysema were used as input variables in the multivariable analysis. In the multivariable analysis, the presence of emphysema [OR = 5.49; 95% CI (2.27–13.25); p < 0.001], was the only independent risk factor for the occurrence of a pneumothorax.

Occurrence of hemoptysis

Hemoptysis occurred in 23 of 213 (10.8%) cases. Two patients (0.9%) required a red blood cell transfusion and intensive care

Table 2. Results of univariable analyses for diagnostic accuracy

Variable	Odds ratio (95% CI)	*p*-value
Gender (male *vs* female)	1.961 (0.807–4.762)	0.137
Age (≤60 *vs* > 60 years)	0.918 (0.386–2.180)	0.918
Target size (cm)	0.339 (0.006–20.596)	0.606
Patient's position (prone *vs* supine)	0.580 (0.217–1.550)	0.278
Target location (upper or middle lobe *vs* lower lobe)	1.355 (0.528–3.476)	0.528
Visibility on fluoroscopy (invisible *vs* visible)	2.489 (1.013–6.117)	0.047
Target characteristics (solid *vs* subsolid)	N/A[a]	1.000[b]
PTTD (≤2 *vs* > 2 cm)	1.158 (0.483–2.774)	0.742
Biopsy method (fine needle aspiration *vs* core biopsy)	2.101 (0.210–21.076)	0.528
Presence of emphysema (absence *vs* presence)	2.788 (0.352–22.055)	0.331

CI, confidence interval; PTTD, pleura to target distance.
[a]One cell had zero value in cross-table analysis.
[b]Fisher's exact test.

unit admission. Hemoptysis resolved spontaneously in all cases with conservative management. In the χ^2 analysis, nodule visibility showed no significant relationship with the occurrence of hemoptysis ($p = 0.383$). Table 4 presents the results of the univariable analyses of the occurrence of hemoptysis. No variable was significantly associated with the occurrence of hemoptysis.

Figure 4. An example of CBCT virtual navigation-guided PTNB for a visible nodule in a 48-year-old male. The preprocedural axial CBCT image shows a 0.7 cm-sized nodule in the right upper lobe (a). The fluoroscopic needle insertion view shows a small nodular opacity, which corresponded to the target location provided by the virtual guidance software (metallic indicator tip; b). The intraprocedural axial CBCT image taken after insertion of the needle shows that the nodule was correctly targeted (c). The pathological diagnosis of the nodule was a metastatic adenoid cystic carcinoma.

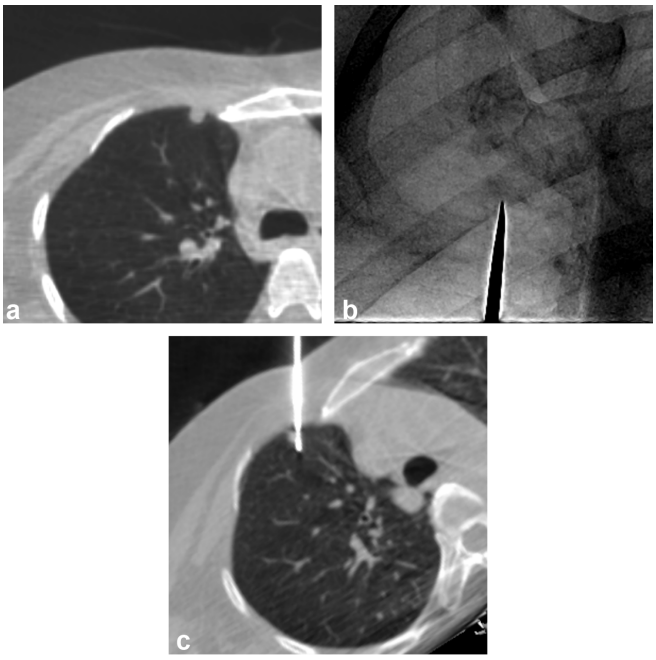

DISCUSSION

In this study, we demonstrated that the diagnostic accuracy of CBCT VN-guided PTNBs for the invisible nodules on real-time

Figure 5. A representative case of CBCT virtual navigation-guided PTNB for an invisible nodule in a 68-year-old female. The preprocedural axial CBCT image shows a nodule, with a maximum diameter of 1.0 cm in the right upper lobe (a). The fluoroscopic needle insertion view shows no definite corresponding opacity in the location marked by the virtual guidance software (metallic indicator tip; b). The intraprocedural CBCT image taken after the needle insertion shows the biopsy needle tip at the lateral aspect of the target (c). The biopsy result was non-neoplastic lung parenchyma. The lesion was diagnosed as a primary lung adenocarcinoma after surgical resection. CBCT, cone-beam computed tomography; PTNB, percutaneous transthoracic needle biopsy.

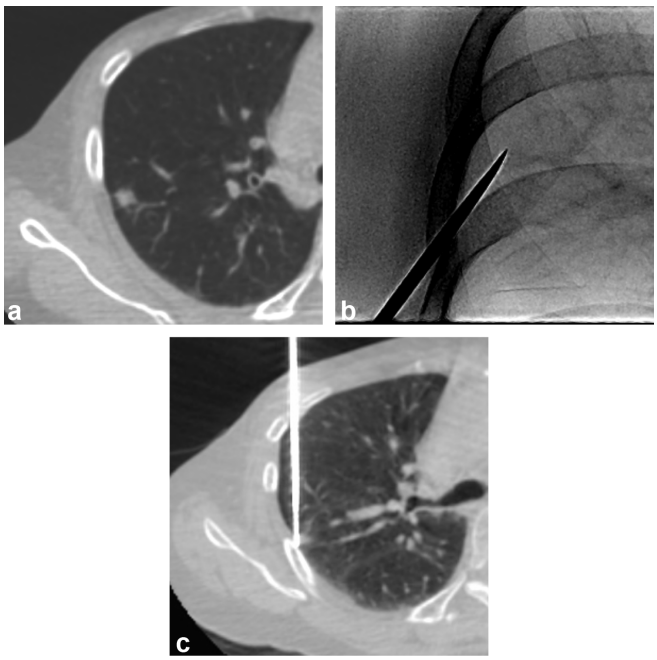

Table 3. Results of univariable analyses for occurrence of pneumothorax

Variable	Odds ratio (95% CI)	*p*-value
Gender (male *vs* female)	1.422 (0.781–2.590)	0.249
Age (≤60 *vs* > 60 years)	2.128 (1.144–3.959)	0.017
Target size (cm)	0.215 (0.016–2.818)	0.242
Patient's position (prone *vs* supine)	1.071 (0.570–2.012)	0.831
Target location (upper or middle lobe *vs* lower lobe)	0.894 (0.480–1.665)	0.724
Visibility on fluoroscopy (invisible *vs* visible)	0.678 (0.360–1.275)	0.227
Target characteristics (solid *vs* subsolid)	0.806 (0.185–4.105)	0.795
PTTD (≤2 *vs* > 2 cm)	1.663 (0.917–3.018)	0.094
Biopsy method (fine needle aspiration *vs* core biopsy)	0.403 (0.055–2.925)	0.369
Presence of emphysema (absence *vs* presence)	5.488 (2.272–13.254)	<0.001

CI, confidence interval; PTTD, pleura -to target distance.

fluoroscopy was 76.7%, which was significantly lower than that for the visible nodules (89.1%). Nodule visibility was a sole independently influencing factor for the correct biopsy results for small (≤1 cm) nodules. However, it was not significantly associated with the biopsy-related complications.

Targeting a small nodule of 1 cm or smaller is challenging. Previous studies reported that small lesion size was a significant predictor of diagnostic failure.[11,15–17] The diagnostic accuracy of CBCT- or CT-guided PTNBs for nodules ≤1 cm ranged from 79 to 98% in the literature.[10,15,17–24] The diagnostic accuracy of biopsy for the subcentimeter-sized, fluoroscopically invisible nodules was 76.7% in our study, which was below the previously reported range. This might be due to the incapability of the fluoroscopy guidance system to track the targets in real-time. Despite the assistance of a VN system and CBCT acquisition during biopsies, real-time visual guidance through fluoroscopy remains essential in targeting small nodules because respiratory movements induce migration of nodules from the planned pathway during the procedure.

Nevertheless, given the high diagnostic accuracy (76.7%) for the invisible nodules in the present study, we believe that PTNBs can be performed for small nodules regardless of their fluoroscopic visibility. In addition, the visibility of a nodule on fluoroscopy cannot be determined until the initiation of the procedure and the majority of nodules (70.4%; 150/213) were actually visible on fluoroscopy. Thus, concerns about invisibility should not preclude CBCT VN-guided PTNBs in cases of small nodules. Furthermore, complication rates were not affected by the fluoroscopic nodule visibility, which implied that PTNBs can be safely performed for the fluoroscopically invisible nodules. A caveat should be noted that the reduced diagnostic accuracy should be considered carefully when interpreting the biopsy results. If a target nodule is invisible on fluoroscopy during the procedure and the subsequent biopsy result points to a non-specific benign lesion, the possibility of a false-negative diagnosis should be considered. Clinicians and radiologists should deliberate on whether to perform a repeat biopsy or surgical resection based on the clinical situation.

A pneumothorax is the most common PTNB-related complication, with a reported incidence of 8.2–62.2%.[11,17–19,22,23,25–27] The frequency of pneumothoraxes in our study was 29.1%, which was within the reported range but was still considerably high. This might have been caused by the small nodule size (≤1 cm) in our study population. A small target size is a well-known risk factor for a PTNB-related pneumothorax.[26,28–31] In our study, the presence of emphysema in the background lung parenchyma was the only independent risk factor for a pneumothorax. Previous studies reported the presence of emphysema as a significant

Table 4. Results of univariable analyses for occurrence of hemoptysis

Variable	Odds ratio (95% CI)	*p*-value
Gender (male *vs* female)	1.723 (0.698–4.256)	0.238
Age (≤60 *vs* > 60 years)	0.488 (0.201–1.183)	0.112
Target size (cm)	0.103 (0.003–3.413)	0.203
Patient's position (prone *vs* supine)	1.916 (0.681–5.393)	0.218
Target location (upper or middle lobe *vs* lower lobe)	1.445 (0.601–3.473)	0.410
Visibility on fluoroscopy (invisible *vs* visible)	1.582 (0.560–4.465)	0.386
Target characteristics (solid *vs* subsolid)	1.188 (0.140–10.115)	0.875
PTTD (≤2 *vs* > 2 cm)	0.688 (0.278–1.699)	0.417
Biopsy method (fine needle aspiration *vs* core biopsy)	N/A[a]	1.000[b]
Presence of emphysema (absence *vs* presence)	N/A[a]	0.084[b]

CI, confidence interval; N/A, not applicable; PTTD, pleura to target distance.
[a]One cell had zero value in cross-table analysis.
[b]Fisher's exact test.

risk factor for PTNB-related pneumothorax.[32,33] Disruption of emphysematous air space can increase airway pressure and prevent rapid sealing of air leaks. Other previously reported risk factors, such as old age,[12] lower lobar location[11,15] or greater lesion depth,[15,29,34] were not statistically significant in our study. This discordance might be due to the small number of included patients and differences in the distribution of nodule size.

In the present study, the frequency of hemoptysis was 10.8%. The result was close to the upper bound of the reported range in the past studies (1.7–14.7%).[27,35–38] This can be explained by the inclusion of only small nodules (≤1 cm) in the present study. A small target size (≤2 cm) has been repeatedly reported as an independent risk factor for biopsy-related hemoptysis.[26,39] In our study, risk factors such as a subsolid nodule type and deep location did not appear to be associated with hemoptysis, in contrast to the findings of previous studies.[11,31,39] The discord in the findings might be attributed to the differences in the size distribution of the lesions.

The visibility of target nodules on real-time fluoroscopy was not a significant risk factor for the occurrence of either a pneumothorax or hemoptysis. We initially assumed that the complication rates would be higher in cases of the invisible nodules because targeting invisible nodules might require more frequent needle redirection and subsequently a longer needle indwelling time. However, the needle indwelling time and total procedure time were not significantly different between the visible and the invisible nodules. The fact that the biopsy-related complications were not associated with the nodule visibility potentiates the usefulness of CBCT VN-guided PTNBs for the subcentimeter-sized nodules.

There were several limitations in this study. First, nodule visibility was assessed retrospectively for the captured images, not on real-time fluoroscopic images. However, we assume that the nodule visibility in both cases will be identical. Furthermore, several possible factors that may impact on diagnostic accuracy and complication rate, such as experience of individual radiologist and degree of inspiration, could not be assessed in this retrospective investigation. To overcome this limitation, prospective recording of nodule visibility during the procedures is required. Second, our study included a relatively small number of patients, as well as a small number of invisible nodules ($n = 63$). Therefore, the possibility of a Type 2 error cannot be excluded, particularly in the analysis of complication rates. A further study with a larger population is warranted.

In conclusion, diagnostic accuracy of CBCT VN-guided PTNB for the invisible nodules on real-time fluoroscopy was 76.7%. Complication rates were not significantly affected by the nodule visibility. Thus, PTNB can be tried safely for the subcentimeter-sized pulmonary nodules regardless of their fluoroscopic visibility.

FUNDING

This research was supported by a grant from the Korea Health Technology R&D Project through the Korea Health Industry Development Institute (KHIDI), funded by the Ministry of Health and Welfare, Republic of Korea (grant number: HC15C3390).

REFERENCES

1. International Early Lung Cancer Action Program Investigators, Henschke CI, Yankelevitz DF, Libby DM, Pasmantier MW, Smith JP, et al. Survival of patients with stage I lung cancer detected on CT screening. *N Engl J Med* 2006; **355**: 1763–71. doi: https://doi.org/10.1056/NEJMoa060476
2. National Lung Screening Trial Research Team, Aberle DR, Adams AM, Berg CD, Black WC, Clapp JD, et al. Reduced lung-cancer mortality with low-dose computed tomographic screening. *N Engl J Med* 2011; **365**: 395–409. doi: https://doi.org/10.1056/NEJMoa1102873
3. Aberle DR, DeMello S, Berg CD, Black WC, Brewer B, Church TR, et al. Results of the two incidence screenings in the national lung screening trial. *N Engl J Med* 2013; **369**: 920–31. doi: https://doi.org/10.1056/NEJMoa1208962
4. National Lung Screening Trial Research Team, Church TR, Black WC, Aberle DR, Berg CD, Clingan KL, et al. Results of initial low-dose computed tomographic screening for lung cancer. *N Engl J Med* 2013; **368**: 1980–91. doi: https://doi.org/10.1056/NEJMoa1209120
5. Callister ME, Baldwin DR, Akram AR, Barnard S, Cane P, Draffan J, et al. British Thoracic Society guidelines for the investigation and management of pulmonary nodules. *Thorax* 2015; **70**(Suppl 2): ii1–ii54. doi: https://doi.org/10.1136/thoraxjnl-2015-207168
6. MacMahon H, Naidich DP, Goo JM, Lee KS, Leung ANC, Mayo JR, et al. Guidelines for management of incidental pulmonary nodules detected on CT images: from the Fleischner Society 2017. *Radiology* 2017; **284**: 228–43. doi: https://doi.org/10.1148/radiol.2017161659
7. McKee BJ, Regis SM, McKee AB, Flacke S, Wald C. Performance of ACR lung-RADS in a clinical CT lung screening program. *J Am Coll Radiol* 2016; **13**(2 Suppl): R25–9. doi: https://doi.org/10.1016/j.jacr.2015.12.009
8. Abi-Jaoudeh N, Fisher T, Jacobus J, Skopec M, Radaelli A, Van Der Bom IM, et al. Prospective randomized trial for image-guided biopsy using cone-beam CT navigation compared with conventional CT. *J Vasc Interv Radiol* 2016; **27**: 1342–9. doi: https://doi.org/10.1016/j.jvir.2016.05.034
9. Choi JW, Park CM, Goo JM, Park YK, Sung W, Lee HJ, et al. C-arm cone-beam CT-guided percutaneous transthoracic needle biopsy of small (≤ 20 mm) lung nodules: diagnostic accuracy and complications in 161 patients. *AJR Am J Roentgenol* 2012; **199**: W322–30. doi: https://doi.org/10.2214/AJR.11.7576
10. Choo JY, Park CM, Lee NK, Lee SM, Lee HJ, Goo JM. Percutaneous transthoracic needle biopsy of small (≤ 1 cm) lung nodules under C-arm cone-beam CT virtual navigation guidance. *Eur Radiol* 2013; **23**: 712–9. doi: https://doi.org/10.1007/s00330-012-2644-6
11. Lee SM, Park CM, Lee KH, Bahn YE, Kim JI, Goo JM. C-arm cone-beam CT-guided percutaneous transthoracic needle biopsy

of lung nodules: clinical experience in 1108 patients. *Radiology* 2014; **271**: 291–300. doi: https://doi.org/10.1148/radiol.13131265
12. Kim JI, Park CM, Lee SM, Goo JM. Rapid needle-out patient-rollover approach after cone beam CT-guided lung biopsy: effect on pneumothorax rate in 1,191 consecutive patients. *Eur Radiol* 2015; **25**: 1845–53. doi: https://doi.org/10.1007/s00330-015-3601-y
13. Mandrekar JN. Measures of interrater agreement. *J Thorac Oncol* 2011; **6**: 6–7. doi: https://doi.org/10.1097/JTO.0b013e318200f983
14. Huang Y, Liu Z, He L, Chen X, Pan D, Ma Z, et al. Radiomics signature: a potential biomarker for the prediction of disease-free survival in early-stage (I or II) non-small cell lung cancer. *Radiology* 2016; **281**: 947–57. doi: https://doi.org/10.1148/radiol.2016152234
15. Hiraki T, Mimura H, Gobara H, Iguchi T, Fujiwara H, Sakurai J, et al. CT fluoroscopy-guided biopsy of 1,000 pulmonary lesions performed with 20-gauge coaxial cutting needles: diagnostic yield and risk factors for diagnostic failure. *Chest* 2009; **136**: 1612–7. doi: https://doi.org/10.1378/chest.09-0370
16. Kothary N, Lock L, Sze DY, Hofmann LV. Computed tomography-guided percutaneous needle biopsy of pulmonary nodules: impact of nodule size on diagnostic accuracy. *Clin Lung Cancer* 2009; **10**: 360–3. doi: https://doi.org/10.3816/CLC.2009.n.049
17. Wallace MJ, Krishnamurthy S, Broemeling LD, Gupta S, Ahrar K, Morello FA, et al. CT-guided percutaneous fine-needle aspiration biopsy of small (< or =1-cm) pulmonary lesions. *Radiology* 2002; **225**: 823–8. doi: https://doi.org/10.1148/radiol.2253011465
18. Choi SH, Chae EJ, Kim JE, Kim EY, Oh SY, Hwang HJ, et al. Percutaneous CT-guided aspiration and core biopsy of pulmonary nodules smaller than 1 cm: analysis of outcomes of 305 procedures from a tertiary referral center. *AJR Am J Roentgenol* 2013; **201**: 964–70. doi: https://doi.org/10.2214/AJR.12.10156
19. DiBardino DM, Yarmus LB, Semaan RW. Transthoracic needle biopsy of the lung. *J Thorac Dis* 2015; **7**(Suppl 4): S304–16. doi: https://doi.org/10.3978/j.issn.2072-1439.2015.12.16
20. Hur J, Lee HJ, Nam JE, Kim YJ, Kim TH, Choe KO, et al. Diagnostic accuracy of CT fluoroscopy-guided needle aspiration biopsy of ground-glass opacity pulmonary lesions. *AJR Am J Roentgenol* 2009; **192**: 629–34. doi: https://doi.org/10.2214/AJR.08.1366
21. Laurent F, Latrabe V, Vergier B, Montaudon M, Vernejoux JM, Dubrez J. CT-guided transthoracic needle biopsy of pulmonary nodules smaller than 20 mm: results with an automated 20-gauge coaxial cutting needle. *Clin Radiol* 2000; **55**: 281–7. doi: https://doi.org/10.1053/crad.1999.0368
22. Ng YL, Patsios D, Roberts H, Walsham A, Paul NS, Chung T, et al. CT-guided percutaneous fine-needle aspiration biopsy of pulmonary nodules measuring 10 mm or less. *Clin Radiol* 2008; **63**: 272–7. doi: https://doi.org/10.1016/j.crad.2007.09.003
23. Yamauchi Y, Izumi Y, Nakatsuka S, Inoue M, Hayashi Y, Mukai M, et al. Diagnostic performance of percutaneous core needle lung biopsy under multi-CT fluoroscopic guidance for ground-glass opacity pulmonary lesions. *Eur J Radiol* 2011; **79**: e85–9. doi: https://doi.org/10.1016/j.ejrad.2011.03.088
24. Chang YY, Chen CK, Yeh YC, Wu MH. Diagnostic feasibility and safety of CT-guided core biopsy for lung nodules less than or equal to 8 mm: a single-institution experience. *Eur Radiol* 2018; **28**: 796–806. doi: https://doi.org/10.1007/s00330-017-5027-1
25. Arslan S, Yilmaz A, Bayramgürler B, Uzman O, Nver E, Akkaya E. CT- guided transthoracic fine needle aspiration of pulmonary lesions: accuracy and complications in 294 patients. *Med Sci Monit* 2002; **8**: CR493–7.
26. Loh SE, Wu DD, Venkatesh SK, Ong CK, Liu E, Seto KY, et al. CT-guided thoracic biopsy: evaluating diagnostic yield and complications. *Ann Acad Med Singapore* 2013; **42**: 285–90.
27. Zhuang YP, Wang HY, Zhang J, Feng Y, Zhang L. Diagnostic accuracy and safety of CT-guided fine needle aspiration biopsy in cavitary pulmonary lesions. *Eur J Radiol* 2013; **82**: 182–6. doi: https://doi.org/10.1016/j.ejrad.2012.09.011
28. Heyer CM, Reichelt S, Peters SA, Walther JW, Müller KM, Nicolas V. Computed tomography-navigated transthoracic core biopsy of pulmonary lesions: which factors affect diagnostic yield and complication rates? *Acad Radiol* 2008; **15**: 1017–26. doi: https://doi.org/10.1016/j.acra.2008.02.018
29. Kazerooni EA, Lim FT, Mikhail A, Martinez FJ. Risk of pneumothorax in CT-guided transthoracic needle aspiration biopsy of the lung. *Radiology* 1996; **198**: 371–5. doi: https://doi.org/10.1148/radiology.198.2.8596834
30. Nour-Eldin NE, Alsubhi M, Emam A, Lehnert T, Beeres M, Jacobi V, et al. Pneumothorax complicating coaxial and non-coaxial CT-guided lung biopsy: comparative analysis of determining risk factors and management of pneumothorax in a retrospective review of 650 patients. *Cardiovasc Intervent Radiol* 2016; **39**: 261–70. doi: https://doi.org/10.1007/s00270-015-1167-3
31. Yeow KM, Su IH, Pan KT, Tsay PK, Lui KW, Cheung YC, et al. Risk factors of pneumothorax and bleeding: multivariate analysis of 660 CT-guided coaxial cutting needle lung biopsies. *Chest* 2004; **126**: 748–54. doi: https://doi.org/10.1378/chest.126.3.748
32. Chami HA, Faraj W, Yehia ZA, Badour SA, Sawan P, Rebeiz K, et al. Predictors of pneumothorax after CT-guided transthoracic needle lung biopsy: the role of quantitative CT. *Clin Radiol* 2015; **70**: 1382–7. doi: https://doi.org/10.1016/j.crad.2015.08.003
33. Schulze R, Seebacher G, Enderes B, Kugler G, Fischer JR, Graeter TP. Complications in CT-guided, semi-automatic coaxial core biopsy of potentially malignant pulmonary lesions. *Rofo* 2015; **187**: 697–702. doi: https://doi.org/10.1055/s-0034-1399648
34. Laurent F, Michel P, Latrabe V, Tunon de Lara M, Marthan R. Pneumothoraces and chest tube placement after CT-guided transthoracic lung biopsy using a coaxial technique: incidence and risk factors. *AJR Am J Roentgenol* 1999; **172**: 1049–53. doi: https://doi.org/10.2214/ajr.172.4.10587145
35. Bladt O, De Wever W. Additional value of CT-fluoroscopic biopsy of pulmonary lesions: a retrospective study of 69 patients. *JBR-BTR* 2006; **89**: 298–302.
36. Jiao deC, Li TF, Han XW, Wu G, Ma J, Fu MT, et al. Clinical applications of the C-arm cone-beam CT-based 3D needle guidance system in performing percutaneous transthoracic needle biopsy of pulmonary lesions. *Diagn Interv Radiol* 2014; **20**: 470–4. doi: https://doi.org/10.5152/dir.2014.13463
37. Yaffe D, Koslow M, Haskiya H, Shitrit D. A novel technique for CT-guided transthoracic biopsy of lung lesions: improved biopsy accuracy and safety. *Eur Radiol* 2015; **25**: 3354–60. doi: https://doi.org/10.1007/s00330-015-3750-z
38. Yildirim E, Kirbas I, Harman A, Ozyer U, Tore HG, Aytekin C, et al. CT-guided cutting needle lung biopsy using modified coaxial technique: factors effecting risk of complications. *Eur J Radiol* 2009; **70**: 57–60. doi: https://doi.org/10.1016/j.ejrad.2008.01.006
39. Song YS, Park CM, Park KW, Kim KG, Lee HJ, Shim MS, et al. Does antiplatelet therapy increase the risk of hemoptysis during percutaneous transthoracic needle biopsy of a pulmonary lesion? *AJR Am J Roentgenol* 2013; **200**: 1014–9. doi: https://doi.org/10.2214/AJR.12.8931